ELSEVIER

Materials Science and Engineering A 447 (2007) 65–70

MATERIALS SCIENCE & ENGINEERING A

www.elsevier.com/locate/msea

Thermomechanical characterization of pure polycrystalline tantalum

D. Rittel [a,*], A. Bhattacharyya [b], B. Poon [b], J. Zhao [b], G. Ravichandran [b]

[a] *Faculty of Mechanical Engineering, Technion, 32000 Haifa, Israel*

[b] *Graduate Aeronautical Laboratories, California Institute of Technology, Pasadena, CA 911125, USA*

Received 16 June 2006; received in revised form 6 August 2006; accepted 12 October 2006

Abstract

The thermomechanical behavior of pure polycrystalline tantalum has been characterized over a wide range of strain rates, using the recently developed shear compression specimen [D. Rittel, S. Lee, G. Ravichandran, Experimental Mechanics 42 (2002) 58–64]. Dynamic experiments were carried out using a split Hopkinson pressure bar, and the specimen's temperature was monitored throughout the tests using an infrared radiometer. The results of the mechanical tests confirm previous results on pure Ta. Specifically, in addition to its significant strain rate sensitivity, it was observed that pure Ta exhibits very little strain hardening at high strain rates. The measured temperature rise in the specimen's gauge was compared to theoretical predictions which assume a total conversion of the mechanical energy into heat ($\beta = 1$) [G.I. Taylor, H. Quinney, Proceedings of the Royal Society of London, vol. A, 1934, pp. 307–326], and an excellent agreement was obtained. This result confirms the previous result of Kapoor and Nemat-Nasser [R. Kapoor, S. Nemat-Nasser, Mech. Mater. 27 (1998) 1–12], while a different experimental approach was adopted here. The assumption that $\beta = 1$ is found to be justified in this specific case by the lack of dynamic strain hardening of pure Ta. However, this assumption should be limited to non-hardening materials, to reflect the fact that strain hardening implies that part of the mechanical energy is stored into the material's microstructure.

Keywords: Tantalum; High strain rate; Thermomechanics; β factor; Temperature

1. Introduction

Tantalum (Ta) is a high-density refractory material, much like tungsten (W), its neighbor in the periodic table. Tantalum is generally used after alloying with other elements, such as tungsten, in order to improve its strength. The static and dynamic mechanical properties of pure polycrystalline Ta have been characterized by a number of authors such as Hoge and Mukherjee [4], Zerilli and Armstrong [5], Lee et al. [6], Duprey and Clifton [7], Kothari and Anand [8] and by Khan and Liang [9]. The literature reports that, for both the quasi-static and dynamic regimes, Ta exhibits a noticeable strain rate sensitivity together with a high ductility to failure. While the strength of pure Ta remains modest, even at large strain rates, its high density makes it an attractive material for applications involving high strain rates at which a large ductility to failure is required when strength requirements remain modest.

A key characteristic of the dynamic deformation of metals is that adiabatic (or nearly) conditions are met, for which the fraction of mechanical energy that cannot be stored into the microstructure (stored energy of cold work [10]), serves to raise the temperature of the material. This thermomechanical coupling effect has been known for long (e.g. Tresca on shear bands [11]). The seminal contribution of Farren and Taylor [12] and Taylor and Quinney [2] showed that the ratio of thermal to mechanical energy (β) evolves with strain but can conveniently be assumed to be taken as 0.9. These measurements were carried out at relatively moderate strain rates, so that one can naturally extend this result to higher strain rates, such as those reached using a split Hopkinson [13] pressure bar apparatus. Measurements of this ratio are relatively scarce, as they necessitate a synchronized measurement of the stress, strain and temperature over a very short duration of time. The most popular temperature measurement device is the infrared detector (e.g. [14]), which has been used as single element, linear array and matrix array [15] to monitor transient temperature changes. The temperature–stress–strain record can then be processed to determine the ratio of the thermal to mechanical energy (subsequently referred to β_{int}) or the ratio of the thermal to mechanical

* Corresponding author. Fax: +972 48295711.
E-mail address: merittel@technion.ac.il (D. Rittel).

0921-5093/$ – see front matter © 2006 Published by Elsevier B.V.
doi:10.1016/j.msea.2006.10.064

power (β_{diff}). The former was determined by Taylor and Quinney [2], while the latter enters the coupled heat equation [16]. These factors have been systematically differentiated and characterized by Rittel [17] for ductile polymers. Parallel work was carried out by Mason et al. [18] for several alloys. All these works reported that the β factors are in fact strain and strain rate sensitive, a fact that implies a separate constitutive equation while reflecting internal microstructural changes that take place during the deformation process.

Concerning Ta, a significant contribution was published by Kapoor and Nemat-Nasser [3], who investigated the thermomechanical behavior of Ta–2.5% W at high strain rates using an infrared detection system. A central point of this work concerned the "reliability" of infrared systems in the sense that the temperature is measured on the surface of the specimen where convection may alter the accuracy of the result. Consequently, these authors performed a series of careful interrupted experiments, varying the initial temperature of the specimen and got to the conclusion that for all practical purposes, one may assume that $\beta_{int} = 1$ for metals and alloys. Such a conclusion, if it applies to all metals, is a significant simplification of the analytical and experimental aspects of the problem and is therefore quite enticing.

Since a joint thermal–mechanical characterization of pure Ta at high strain rates is still missing, the present work has the two following goals: characterize the mechanical behavior of pure polycrystalline Ta over a large range of strain rates and characterize the extent of the thermomechanical coupling to define limits of validity for the assumption that $\beta_{int} = 1$.

The paper is organized as follows: the material, specimens and experimental conditions are introduced in Section 2. Special emphasis is put on the calibration of the infrared temperature measurement system, especially on the influence of mechanical strain on the surface emissivity of Ta. Section 3 presents typical results on the mechanical properties of this material, including characteristic temperature evolution profiles during the test. Section 4 discusses the results for both the mechanical and thermal aspects of this work, followed by concluding remarks.

2. Experimental

2.1. Materials

Two pure polycrystalline Ta (composition given in Table 1) were purchased as cylindrical, 1/4 in. diameter bars. One bar was annealed ("annealed") while the other bar did not undergo any heat treatment after the extrusion process ("as-received").

2.2. Specimens and data reduction

Two kinds of specimens were machined from the bars and used throughout this study. The first kind consists of cylinders, 6.33 mm diameter and length. The second kind of specimens consists of shear compression cylindrical specimens (SCS [1,19–23]). For the sake of brevity, it will only be mentioned that this specimen allows a shear dominant type of deformation in its gauge section, and it can be used for both quasi-static and dynamic tests using the same data reduction algorithm. The following characteristic dimensions were used for the SCS: 6.33 mm diameter (D), 10 mm high, 1.05 mm gauge width and 2.05 mm gauge thickness (t). The exact dimensions of each specimen were checked individually prior to testing.

Table 1
Composition of the Ta used in this study (weight percent)

Element	Composition (ppm)
C	<10
O	<10
N	<10
H	<5
Nb	19
Fe	<3
Ni	<1
Si	<10
Ti	<1
W	6
Mo	<2
Ta	99.99%

Data reduction for the SCS specimens was carried out as detailed in Dorogoy and Rittel [22,23]. This includes a detailed finite element study of the specimen to determine the K coefficients that relate the loads and displacements to equivalent stresses and strains in the gauge section. While three K coefficients have been used in the past for the investigated materials, it was found that a higher order polynomial approximation provides a better representation of the stresses and strains in the gauge section [24], so that the following data reduction equations were used in this study:

$$\varepsilon_e = \varepsilon_y + K_3\frac{d-d_y}{h} + K_4\left(\frac{d-d_y}{h}\right)^2 \quad (1)$$

$$\sigma_e = K_1(1-K_2\varepsilon_e)\frac{P}{Dt} \quad (2)$$

where d is the vertical prescribed displacement of the gauge section and P is the applied load. The terms ε_Y and d_y correspond to the strain and displacement values at the yield point. The K parameters were determined to be $K_1 = 0.92$, $K_2 = 0.15$, $K_3 = 0.96$ and $K_4 = -0.55$, respectively [24]. The validity of Eqs. (1) and (2) can be finally assessed by comparing stress–strain curves obtained for cylindrical and SCS specimens, as shown in the sequel.

2.3. Mechanical and thermal experimental setups

Quasi-static compression tests (cylinders and SCS) were performed on a standard servo-hydraulic testing machine (MTS Model No. 11019). The machine compliance was taken into account during data reduction. The dynamic compression experiments were carried out on a 12.7 mm diameter Kolsky bar made of C300 Maraging steel. Data were reduced according to the well-known equations relating the stresses and strains to the incident, reflected and transmitted strain signals. Wave dispersion was corrected too, according to the guidelines of Lifshitz

and Leber [25] by means of a homemade software ("Twobar" [26]). Finally, specimen equilibrium (usually assumed, but not necessarily verified) was carefully verified in each test, by comparing the applied forces on each side of the specimen.

The infrared radiometric setup consists of a parabolic mirror and a single element, liquid N_2 cooled HgCdTe detector and its matching amplifier (Judson PA-100). Since a single detector was used, the temperature of a small area can be measured. The size of this area depends on the active area of the detector, which is 100 μm × 100 μm in this case. The imaging system (Newtonian) comprises a concave mirror with a radius of curvature of 70 mm, and a 45° reflecting mirror placed at the focus of the concave mirror. The area magnification was set to approximately 1. The overall setup is shown in Fig. 1.

In order to determine the temperature of the gauge section from the infrared signal, a small K-type thermocouple was tightly inserted at mid thickness of the gauge section of a dummy SCS specimen. Calibration consisted of heating the specimen in a separate furnace, inserting it rapidly between the bars and simultaneously recording the signal from the thermocouple and that of the infrared detector, as the specimen cooled down to room temperature. The calibrations were repeated several times, right before dynamic testing, to insure repeatability. Considerable care was exercised concerning accurate and repeatable specimen positioning between the bars, as well as accurate focusing of the IR system on the gauge section. A great advantage of the SCS is that the part of the gauge that faces the IR system remains relatively flat with very limited bulging during the deformation process, thus limiting de-focusing of the system related to depth of field considerations. However, it is well known that some surface texture may develop during the deformation process, which affects the optical characteristics of the investigated material. This eventuality was also taken into account by Kapoor and Nemat-Nasser [3]. Therefore, calibrations were performed using undeformed specimens, and also a specimen that was strained by 0.4. Typical results of these calibrations are reported in the next section.

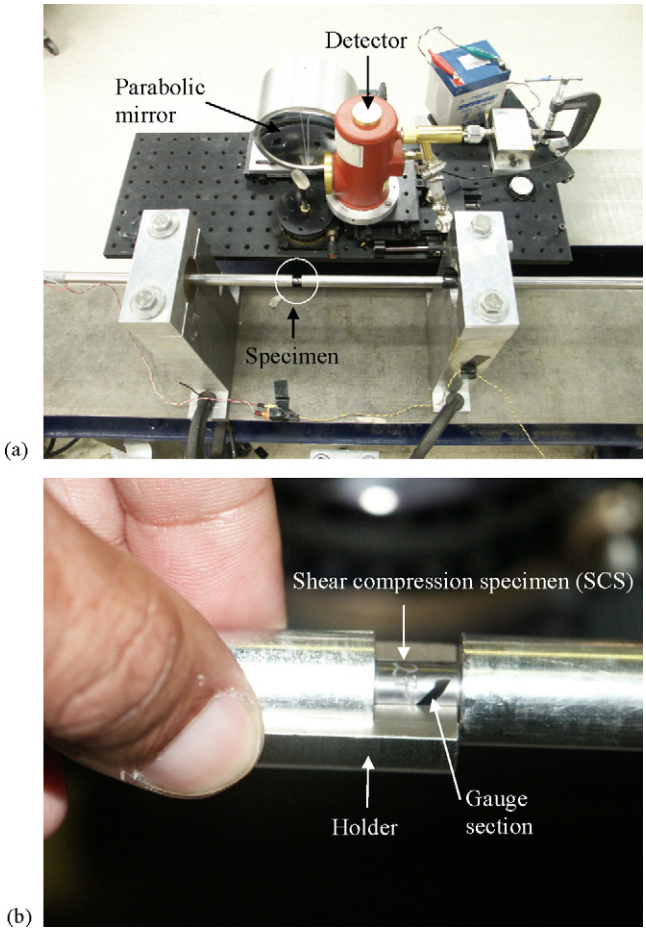

Fig. 1. (a) Experimental setup. (b) The SCS is initially positioned and centered between the bars, by means of a special holder to. At the time of the test, the holder is taken away and the gauge section faces the IR detector.

3. Experimental results

3.1. Mechanical results

Typical stress–strain curves for quasi-statically deformed annealed and as-received Ta samples are shown in Figs. 2 and 3, respectively. Fig. 2 compares a cylindrical and an SCS specimen that were tested at a similar strain rate. It can be noted that the two specimen geometries yield results that compare quite well, this validating the choice of coefficients used to reduce the SCS data. One should also note that, for quasi-statically compressed cylindrical specimens, reliable data are limited to strains that do not exceed 0.15 as barreling gradually develops at higher strains. Fig. 3 (comprising both cylinders and SCS) illustrates first of all the high strain rate sensitivity of pure Ta, even in the quasi-static regime. Finally, a comparison of the two figures shows that the annealed grade has a significantly higher strain hardening capacity than the as-received, and this result is quite expected.

Typical dynamic stress–strain curves are shown in Figs. 4 and 5 for the annealed and as-received Ta samples, respectively. A comparison of these figures with Figs. 3 and 4 shows

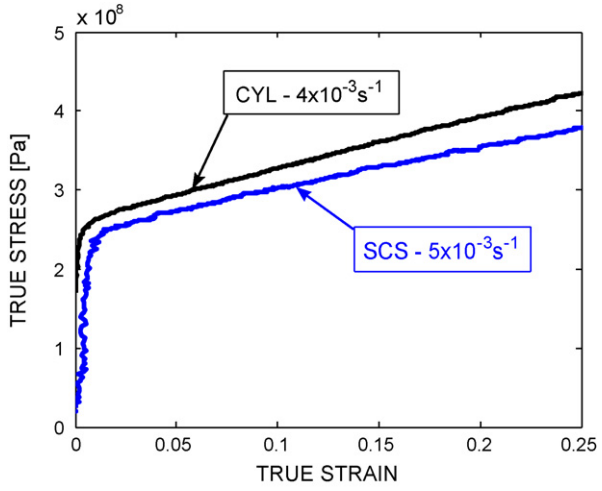

Fig. 2. Quasi-static stress–strain curves: annealed Ta and cylindrical and SCS specimens.

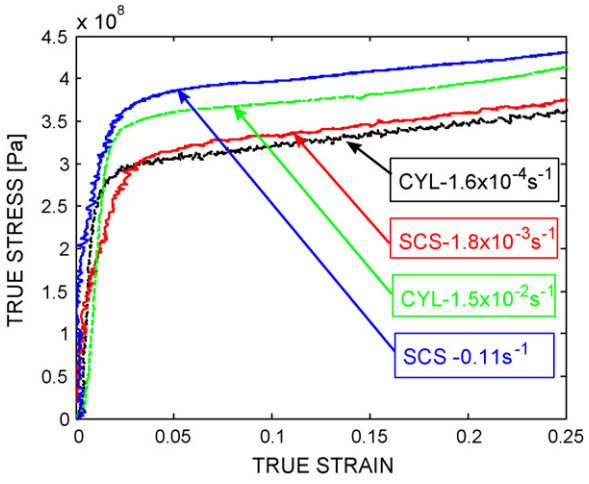

Fig. 3. Quasi-static stress–strain curves: as-received Ta and cylindrical and SCS specimens.

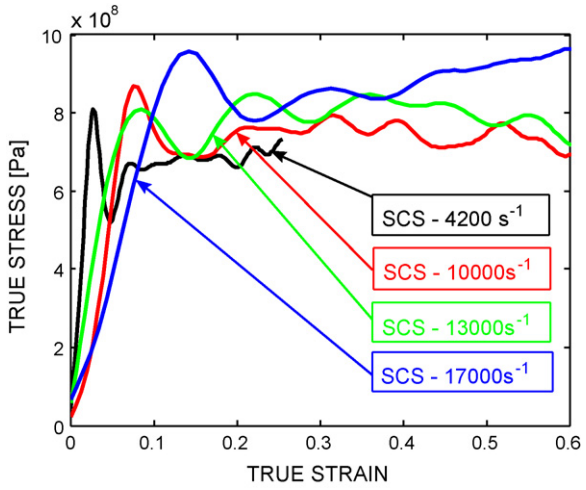

Fig. 5. Dynamic stress–strain curves: as-received Ta. Note the lack of strain hardening.

that the dynamic flow stress Ta is far higher than the quasi-static, irrespective of the initial condition. However, the material looses its strain hardening capacity at the high rates and flows in what appears to be a perfectly plastic mode, again irrespective of the initial condition (the oscillations that appear on the graph are characteristic of dynamic tests involving wave reflections in the specimen [23]).

Finally, Fig. 6 illustrates the degree of strain rate sensitivity of the two grades, in the form of a semi-logarithmic plot of the flow stress at $\varepsilon_t = 0.1$ as a function of the strain rate. The range of investigated strain rates is quite large, as it reaches $\dot{\varepsilon} = 17,000\,s^{-1}$. This figure confirms the high rate sensitivity of Ta, irrespective of its initial condition. It can also be noted that contrary to steel, for instance, the rate sensitivity is evident all across the range of strain rates, rather than from a given strain rate and thereon. It can also be noted, that from a practical point of view, the two grades of pure Ta exhibit identical flow stresses in the high strain rate regime.

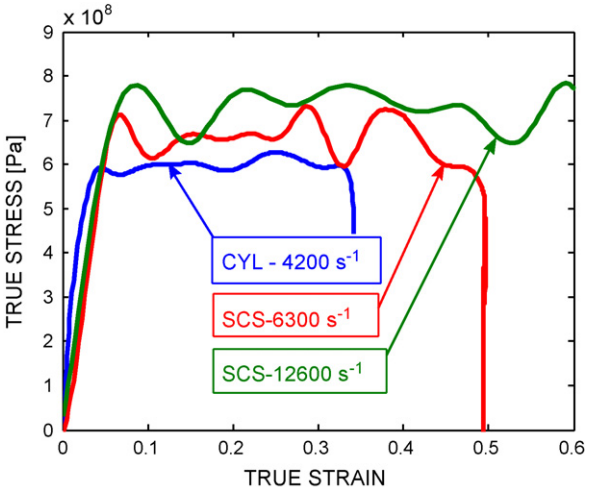

Fig. 4. Dynamic stress–strain curves: annealed Ta. Note the lack of strain hardening.

3.2. IR system calibration

Calibration of the IR system is a crucial step to insure reliable data. The basic procedure was detailed in Section 1. Practical calibration steps included a series of five or more calibration experiments carried out in a row, before each series of experiments. The detector voltage–thermocouple temperature data of each calibration experiment were all gathered into a single set of data and regression analysis was then applied to determine a best-fit equation. As mentioned, calibrations were performed on an undeformed SCS and on a specimen that had been deformed to $\varepsilon_t = 0.4$. Fig. 7 shows typical calibration curves. These curves show that deformation does not have a pronounced effect on the calibration curve, by ways of gauge surface alteration. It was nevertheless decided to process all the thermal signals according to the calibration obtained from the deformed specimen.

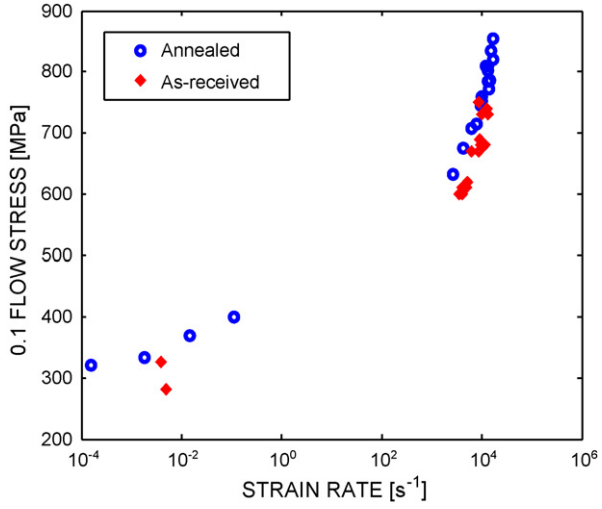

Fig. 6. Semi-logarithmic plot of the flow stress at $\varepsilon_{tot} = 0.1$ as a function of the strain rate. Tantalum is strain rate sensitive throughout the range of investigated strain rates. The annealed and as-received grades have similar flow properties at high strain rates.

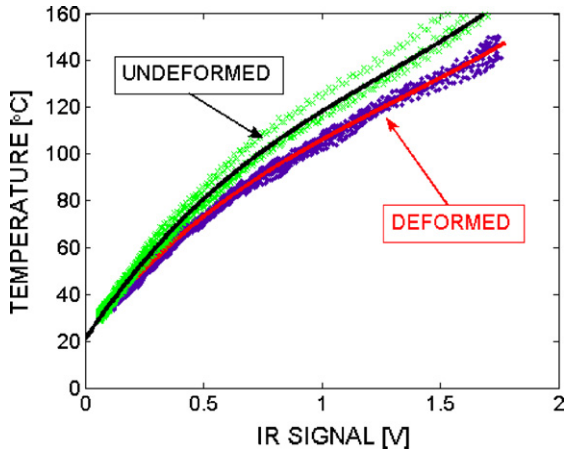

Fig. 7. Typical calibration curves relating the temperature to IR signal. The solid lines show the best fit for several sets of experiments carried out on undeformed and deformed ($\varepsilon_{tot} = 0.4$) SCS specimens. The deformed calibration line was used to process the thermal data.

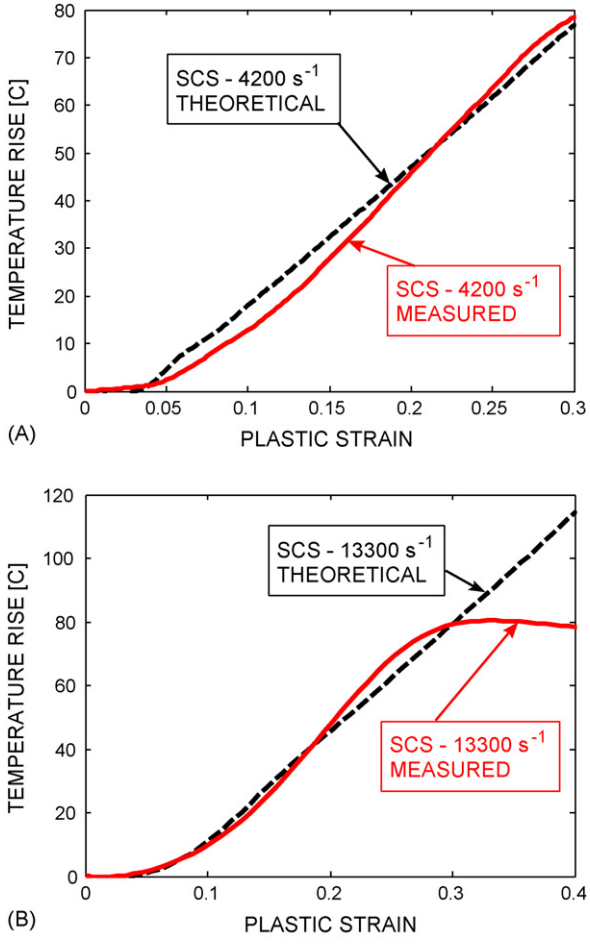

Fig. 8. Typical recordings of the temperature rise at intermediate (A) and high (B) strain rates: as-received Ta. The dashed line indicates the theoretically predicted temperature rise corresponding to $\beta_{int} = 1$. Note the excellent agreement between the experimental and theoretical results. The flattening out of the IR signal in (B) is related to motion of the specimen and is an experimental artifact.

3.3. Thermal results

Typical plots of the temperature rise as a function of the plastic strain are shown in (Fig. 8A and B), for the as-received Ta, at two very different strain rates. On these curves, a theoretical estimate of the temperature rise has been superimposed, based on the assumption that $\beta_{int} = 1$. One may note that the temperature rise is insignificant for strain levels of up to 0.05. This observation may be related to the calibration (Fig. 7) which shows a small sensitivity to small temperature changes around room temperature. This figure shows that, on the average, the measured and calculated temperature rises are quite similar, even if some small deviations are noticeable. The absolute precision of the measurement (namely the calibration curve) cannot be accurately estimated here, and these deviations may indeed be related to the calibration curve, while there is a clear trend for the measured temperature rise to align with the calculated one. Fig. 8B shows a thermal plateau that was observed in several experiments. Considering the very small width of the sheared gauge over which the detector is focused, it is reasonable to assume that the small specimen motion during the deformation is likely to bring colder parts into focus, thus causing the observed plateau or even an apparent temperature decrease in some cases. This is an experimental artifact so that the observed plateau is not a true thermal effect. On an overall level, Fig. 8 reveals an excellent agreement between the measured and the calculated temperature rise, irrespective of the strain rate. In other words, one may conclude that for practical purposes, all of the mechanical energy of pure Ta transforms into heat, almost from the onset of plastic deformation.

4. Discussion

The thermomechanical behavior of pure Ta has been characterized over a wide range of strain rates, using the shear compression specimen. Two grades of material were used in this study. Our results confirm the high strain rate sensitivity of this material which is observable even in the quasi-static regime. These results are in perfect agreement with previous results on pure Ta. A very important feature of the high rate flow of annealed Ta is that the material flows without noticeable hardening. The observed lack of hardening is a direct indication that this material cannot store internal energy through generation and rearrangement of defects, since this would necessarily imply strain hardening. This point has a decisive impact on the thermal evolution as discussed next.

Temperature monitoring can be considered as accurate, since great care was exercised to insure optimal specimen positioning with respect to the detector and high accuracy, and mostly repeatability of the infrared recording and data processing. Inspite of the minor influence of the strain on the infrared signal, it was decided to use the calibration obtained from a deformed specimen for all the experiments, not to overlook the contribution of the deformation process. Here, the great advantage of the planar gauge of the SCS should be emphasized for a measurement in which focusing issues can induce significant errors in the measurement.

The thermal recordings of high rate experiments all point out to the fact that the recorded temperature rise corresponds to that which would be expected from a total transformation of the mechanical energy into heat, i.e. $\beta_{int} = 1$, within experimental error. These results are in agreement with those of Kapoor and Nemat-Nasser [3] who characterized a slightly alloyed Ta material. However, these authors got to this conclusion through interrupted experiments and specimen reheating while their direct recording pointed to what they view as erroneous results. One of their claims concerned the reliability of IR monitoring when heat convection may obscure the result. These authors made a careful assessment of the influence of the strain on the recorded IR signal and their conclusions match ours. Yet, while our results exactly match their conclusion, the experiments carried out in this work bring to the conclusion that on the average, $\beta_{int} = 1$ indeed, but in a straightforward manner, so that the thermal results presented here can be viewed as reliable.

One last point to be discussed concerns the generality of the assumption of $\beta_{int} = 1$. One point to be noted is that Ta does not exhibit significant strain hardening at high loading rates. As mentioned, this means that mechanical energy cannot be stored in the material, or in other words, all the mechanical energy is dissipated as heat, from an energy balance. Otherwise stated, this means that $\beta_{int} = 1$ for the specific case of Ta studied here, or any other material with a similar lack of hardening. At the risk of stating the obvious, extending this assumption to all metals seems to overlook hardening issues which divert a fraction of mechanical energy by storing it. It is therefore concluded that for the specific case of Ta and similar ideally plastic materials, one can safely assume that $\beta_{int} = 1$, thus greatly simplifying the thermomechanical problem. For all the other cases of strain hardening metals, this assumption is of an upper bound character, in terms of temperature rise calculation.

5. Conclusions

- Pure polycrystalline Ta is a highly strain rate sensitive material, whether annealed or as-received, in accord with previous reports.
- At low strain rates, annealed Ta exhibits more prominent strain hardening than in the as-received condition.
- Dynamic flow of Ta is characterized by a lack of strain hardening, similar to ideally plastic flow.
- The assumption of a total thermomechanical conversion ($\beta_{int} = 1$) has been verified experimentally, in a straightforward manner, and shown to be totally justified for pure Ta.
- The assumption of a total thermomechanical conversion ($\beta_{int} = 1$) cannot be generalized to materials that show strain hardening at high strain rates, since this overlooks energy storage at the microstructural level.

Acknowledgements

The authors gratefully acknowledge the support of the Department of Energy through Caltech's ASCI ASAP Center for the Simulation of the Dynamic Response of Materials. Dr. A. Dorogoy is acknowledged for his numerical simulations of the SCS.

References

[1] D. Rittel, S. Lee, G. Ravichandran, Exp. Mech. 42 (2002) 58–64.
[2] G.I. Taylor, H. Quinney, Proceedings of the Royal Society of London, vol. A, 1934, pp. 307–326.
[3] R. Kapoor, S. Nemat-Nasser, Mech. Mater. 27 (1998) 1–12.
[4] K.G. Hoge, A.K. Mukherjee, J. Mater. Sci. 12 (1977) 1666–1672.
[5] F.J. Zerilli, R.W. Armstrong, J. Appl. Phys. 68 (1990) 1580–1591.
[6] B.-J. Lee, K.S. Vecchio, S. Ahzi, S. Schoenfeld, Metall. Mater. Trans. A 28A (1997) 113–122.
[7] K.E. Duprey, R.J. Clifton, AIP Conference Proceedings, vol. 429, 1988, pp. 475–478.
[8] M. Kothari, L. Anand, J. Mech. Phys. Solids 46 (1998) 51–83.
[9] A.-S. Khan, R. Liang, Int. J. Plast. 15 (1999) 1089–1109.
[10] M.B. Bever, D.L. Holt, A.L. Titchener, in: B. Chalmers, J.W. Christian, T.B. Massalski (Eds.) Prog. Mater. Sci. 17 (1973) 5–88.
[11] H. Tresca, Annales du Conservatoire des Arts et Métiers (1879) 41.
[12] W.S. Farren, G.I. Taylor, Proceedings of the Royal Society of London, vol. CVII, 1925, pp. 422–451.
[13] H. Kolsky, Proceedings of the Royal Society of London, vol. 62-B, 1949, pp. 676–700.
[14] K.A. Hartley, J. Duffy, R.H. Hawley, J. Mech. Phys. Solids 35 (1986) 283–301.
[15] A.T. Zehnder, P.R. Guduru, A.J. Rosakis, G. Ravichandran, Rev. Sci. Instrum. 71 (2000) 3762–3768.
[16] B.A. Boley, J.H. Weiner, Theory of Thermal Stresses, John Wiley and Sons, New York, NY, 1960.
[17] D. Rittel, Mech. Mater. 31 (1999) 131–139.
[18] J.J. Mason, A.J. Rosakis, G. Ravichandran, Mech. Mater. 17 (1994) 135–145.
[19] D. Rittel, S. Lee, G. Ravichandran, Mech. Mater. 34 (2002) 627–642.
[20] D. Rittel, R. Levin, A. Dorogoy, Metall. Mater. Trans. 35A (2004) 3787–3795.
[21] M. Vural, D. Rittel, G. Ravichandran, Metall. Mater. Trans. 34A (2003) 2873–2885.
[22] A. Dorogoy, D. Rittel, Exp. Mech. 45 (2005) 167–177.
[23] A. Dorogoy, D. Rittel, Exp. Mech. 45 (2005) 178–185.
[24] A. Dorogoy, 2005, private communication.
[25] J.M. Lifshitz, H. Leber, Int. J. Impact Eng. 15 (1994) 723–733.
[26] D. Rittel, Twobar: A Program To Process Split Hopkinson Pressure Bar Data, Technion, 1994.